doi:10.1016/S0022-2836(03)00040-8 *J. Mol. Biol.* (2003) **326**, 1489–1501

JMB

Available online at www.sciencedirect.com

SCIENCE DIRECT®

On the Interaction Between gp41 and Membranes: The Immunodominant Loop Stabilizes gp41 Helical Hairpin Conformation

Sergio G. Peisajovich[1], Lior Blank[1], Raquel F. Epand[2] Richard M. Epand[2] and Yechiel Shai[1]*

[1]*Department of Biological Chemistry, Weizmann Institute of Science, Rehovot 76100 Israel*

[2]*Department of Biochemistry McMaster University Health Sciences Centre, Hamilton Ont., Canada L8N 3Z5*

**Corresponding author*

gp41 is the protein responsible for the process of membrane fusion that allows primate lentiviruses (HIV and SIV) to enter into their host cells. gp41 ectodomain contains an N-terminal and a C-terminal heptad repeat region (NHR and CHR) connected by an immunodominant loop. In the absence of membranes, the NHR and CHR segments fold into a protease-resistant core with a trimeric helical hairpin structure. However, when the immunodominant loop is not present (either in a complex formed by HIV-1 gp41-derived NHR and CHR peptides or by mild treatment with protease of recombinant constructs of HIV-1 gp41 ectodomain, which also lack the N-terminal fusion peptide and the C-terminal Trp-rich region) membrane binding induces a conformational change in the gp41 core structure. Here, we further investigated whether covalently linking the NHR and CHR segments by the immunodominant loop affects this conformational change. Specifically, we analyzed a construct corresponding to a fragment of SIVmac239 gp41ectodomain (residues 27–149, named e-gp41) by means of surface plasmon resonance, Trp and rhodamine fluorescence, ATR-FTIR spectroscopy, and differential scanning calorimetry. Our results suggest that the presence of the loop stabilizes the trimeric helical hairpin both when e-gp41 is in aqueous solution and when it is bound to the membrane surface. Bearing in mind possible differences between HIV-1 and SIV gp41, and considering that the gp41 ectodomain constructs analyzed to date lack the N-terminal fusion peptide and the C-terminal Trp-rich region, we discuss our observations in relation to the mechanism of virus-induced membrane fusion.

Keywords: HIV-cell entry; conformational change; membrane fusion

Introduction

gp120 and gp41 are the envelope glycoproteins that mediate the entry of primate lentiviruses, human immunodeficiency virus (HIV) and simian immunodeficiency virus (SIV), into their host cells. They are synthesized as an inactive precursor that is cleaved during the transport to the plasma membrane of the infected cell. gp120, which is non-covalently attached to the integral membrane subunit gp41, mediates the binding to the target cell receptor CD4[1] and to other co-receptors.[2,3] The native conformation of gp41 is metastable and is stabilized by gp120. As a result of the interaction with the target cell receptors, gp41 undergoes a conformational change, the first step in a process that will lead to membrane merging. At the N terminus of gp41, a stretch of about 15 hydrophobic

Abbreviations used: ATR-FTIR, attenuated total reflection Fourier-transformed infrared spectroscopy; βOG, *n*-octyl-β-D-glucopyranoside; DMF, dimethylformamide; DOPC, dioleoylphosphatidylcholine; GuHCl, guanidinium hydrochloride; HIV and SIV, human and simian immunodeficiency virus; LUV, large unilamellar vesicles; NHR and CHR, N-terminal and C-terminal heptad repeat regions; PBS, phosphate buffered saline; PC, phosphatidylcholine; Rho, rhodamine; RP-HPLC, reverse phase-high performance liquid chromatography; RU, response units of the resonance signal; SPR, surface plasmon resonance; TEA, triethylamine.

E-mail address of the corresponding author: yechiel.shai@weizmann.ac.il

0022-2836/03/$ - see front matter

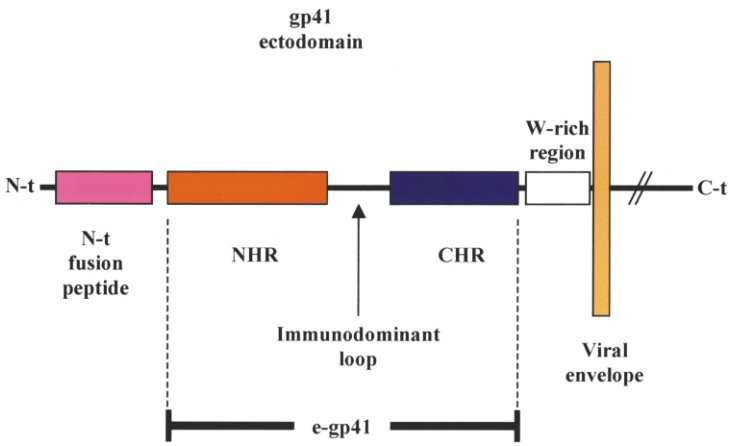

Figure 1. A representation of gp41.

residues, named the fusion peptide,[4,5] is believed to insert into and destabilize the membrane, thus facilitating fusion.[6] Consecutive to the fusion peptide and preceding the transmembrane domain, two heptad repeat regions (NHR and CHR, respectively) have been identified.[7] Indeed, protease treatment of gp41 led to the identification of a protease-resistant core formed by a 3:3 complex of NHR and CHR molecules.[8,9] Crystal structures of the HIV-1 gp41-derived, protease-resistant core,[10,11] as well as the solution NMR structure of a segment of SIV gp41 ectodomain determined at pH 3.0,[12] all lacking the fusion peptide, show that, in the absence of lipid membranes, three NHR molecules fold into a central trimeric coiled-coil, against which three antiparallel helices formed by three CHR molecules are packed. In the NMR structure, each pair of NHR/CHR molecules is connected by the immunogenic, protease-sensitive loop that reverses the polypeptide chain. This trimeric helical hairpin structure is thought to form at a late stage during the membrane fusion process.[10,11] Synthetic peptides that partially overlap the CHR were found to be potent inhibitors of gp41-mediated membrane fusion.[13] The analogy between the structural organizations of gp41 and hemagglutinin, the fusion protein of influenza virus,[14,15] and the inhibitory activity of CHR-derived peptides led to the postulate of a "pre-hairpin intermediate" in gp41-induced membrane fusion, in which the N-terminal coiled-coil is formed, but the C-terminal helices are not packed.[10,11] At this stage, the C-peptide inhibitors could bind to the exposed coiled-coil, thus preventing the subsequent refolding and blocking fusion.[16]

Although it was initially believed that gp41 interacts with the membrane solely by means of the N-terminal fusion peptide and the transmembrane domain, it has been shown recently that gp41 constructs lacking these two segments bind to the surface of phospholipid bilayers.[17,18] In line with this, regions apart from N-terminal fusion peptides, in the ectodomain of other viral fusion proteins have been shown to interact with membranes.[19,20–23] Furthermore, it has been reported that the interaction with the lipid bilayers has structural consequences on HIV-1 gp41.[17] Specifically, it has been shown that a complex of synthetic peptides corresponding to the HIV-1 gp41-derived protease-resistant core dissociates upon membrane binding.[17] Furthermore, when recombinant constructs of HIV-1 gp41 ectodomain, lacking the fusion peptide and the pre-transmembrane Trp-rich region, are treated with proteases in the presence of membranes (conditions that, in the absence of membranes yield the NHR and CHR peptides that form the protease-resistant core), no resistant peptides remain.[17] These observations suggested the hypothesis that, upon interactions with lipid bilayers, HIV-1 gp41 undergoes an additional conformational change in which the trimeric helical hairpin opens.[17]

The experiments done with synthetic peptides corresponding to the HIV-1 gp41 NHR and CHR regions that form the helical hairpin showed that, when the NHR and the CHR are not covalently connected by the immunogenic loop, membrane binding results in the dissociation of the complex. In the experiments done with recombinant constructs, in which the NHR and CHR regions were initially connected by the loop, protease treatment was used to probe the protein conformation. Since the HIV-1 gp41 constructs were incubated with membranes in the presence of the protease (although the protease was added after membrane binding),[17] it is possible that the conformational change observed occurred only after the protease had removed the loop. Thus, we still do not know whether the conformational change is similar when the loop is covalently linking the NHR and the CHR together.

Here, we performed a series of experiments with constructs corresponding to a segment from SIV gp41 ectodomain (residues 27–149, named e-gp41, see Figure 1) lacking the fusion peptide and the pre-transmembrane Trp-rich region, to further investigate whether membrane binding induces a conformational change in gp41. Specifically, we analyzed possible changes in e-gp41 structure upon interaction with lipid bilayers by means of Trp and rhodamine (Rho) fluorescence spectroscopy, surface plasmon resonance (SPR), attenuated

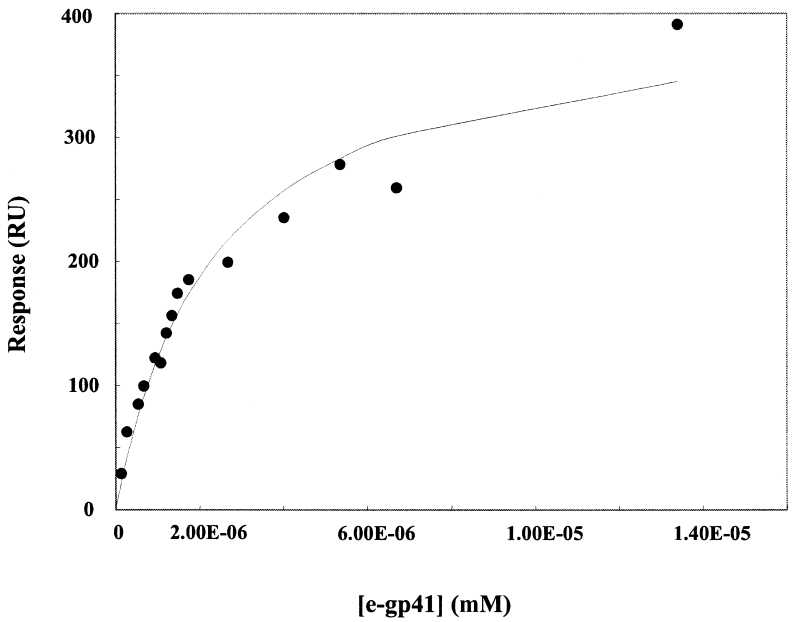

Figure 2. Determination of the membrane-binding affinity constant (K_A) by SPR. A model PC monolayer was deposited on an HPA sensor chip. Analysis of the protein–lipid binding event was performed from a series of sensograms collected at several different concentrations of e-gp41 (in the range from 134 nM to 13.4 μM) in 50 mM sodium formate (pH 3.0), at 25 °C. The sensograms reached equilibrium during sample injection; therefore the affinity constant could be calculated from the relationship between the equilibrium binding response and the concentration of protein (shown here), using a steady-state affinity model. Symbols: experimental data, filled circles; fitted curve, continuous line.

total reflection Fourier-transformed infrared spectroscopy (ATR-FTIR), and differential scanning calorimetry. The results are discussed in relation to the mechanism of gp41-induced membrane fusion.

Results

Membrane partition of e-gp41

e-gp41 (residues 27–149 of SIVmac239 ectodomain, see Figure 1) has been shown to qualitatively bind to PC membranes by means of the e-gp41 Trp/dansylated phospholipids energy transfer and by changes in the e-gp41 Trp fluorescence.[18] However, no quantitative analysis of membrane binding has been reported to date. Here, we measured the affinity constant (K_A) of e-gp41/membrane interaction by SPR in a BIAcore 3000 instrument using a PC monolayer deposited on an HPA chip. Analysis of the e-gp41-lipid binding event was performed from a series of sensograms collected at several different concentrations of e-gp41 (in the range from 134 nM to 13.4 μM). SIV e-gp41 is known to aggregate at neutral pH,[24] presumably *via* protein–protein interactions that involve the loop connecting the N and C-terminal helical segments. Consequently, studies at neutral pH can be done only after removal of the connecting loop (either by genetic manipulation or by treatment with protease). On the contrary, e-gp41 structure and oligomerization state are not affected by low pH.[24] Thus, in order to prevent aggregation without removing the loop, we performed this experiment (and others, as indicated) at low pH. The sensograms reached equilibrium during sample injection; therefore, the affinity constant was calculated from the relationship between the equilibrium binding response and the protein concentration (Figure 2), using a steady-state affinity model. The derived affinity constant (K_A) is $4.33 \times 10^5\ M^{-1}$ and the corresponding ΔG is -10.1 kcal/mol. This value is similar to those obtained for other polypeptides that bind to the membrane surface.[17,25]

Determination of membrane-induced changes in the oligomeric state of e-gp41 by Trp fluorescence

In aqueous solution at low pH, e-gp41 monomers and trimers are in equilibrium, with an association constant, K_a, of 3.1×10^{11}.[24] Here, we investigated whether membrane-binding induces a conformational change in e-gp41 that affects its oligomerization state. The hypothesis was that, considering that the complex formed by the NHR and CHR peptides dissociates upon membrane binding, it could be possible that membrane-binding induces the dissociation of e-gp41 trimers into monomeric species. Binding of monomeric e-gp41 to PC liposomes (at 0.2 μM more than 90% of the protein is monomeric) results in an increase of the e-gp41 Trp fluorescence, whereas binding of e-gp41 trimers (at 5 μM more than 90% of the protein is trimeric) results in a decrease of Trp fluorescence.[18] Thus, we compared the fluorescence upon membrane binding of e-gp41 monomers and trimers, after normalizing the intensity to the concentration. If e-gp41 trimers dissociate upon binding, their final fluorescence should resemble that of the monomers. On the contrary, if they do not dissociate, the final level of the monomer and trimer fluorescence does not need to be similar. As observed in Figure 3, the intensity of fluorescence at concentrations at which there are mainly trimers differs substantially from the values obtained al low concentrations, where there are mainly monomers. Thus, we conclude that membrane binding

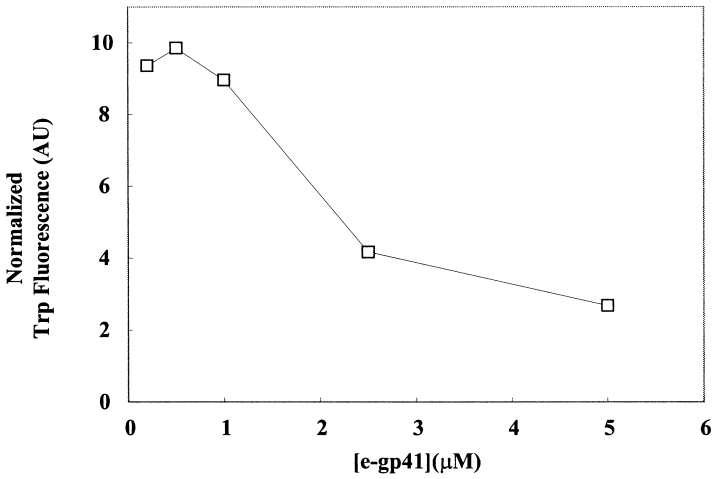

Figure 3. Comparison of the Trp fluorescence of membrane-bound e-gp41 monomers and trimers. The Trp emission spectra of membrane-bound e-gp41 (0.2 μM, 0.5 μM, 1.0 μM, 2.5 μM, and 5.0 μM, [e-gp41]/[lipid] ratio of 1:1000) in 50 mM sodium formate (pH 3.0), were recorded with excitation set at 280 nm (4 nm slit-widths) and emission between 300 nm and 400 nm at 25 °C. The final fluorescence intensity was normalized according to the concentration to allow direct comparison of the different concentrations.

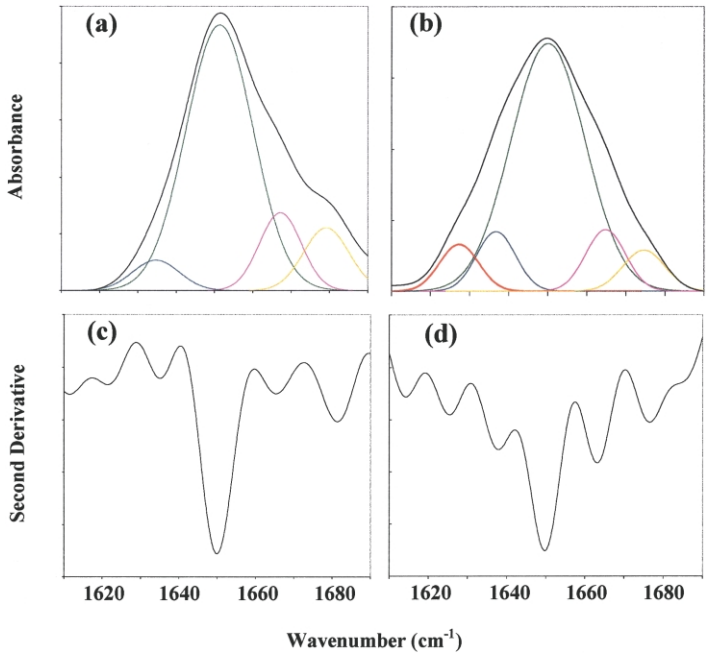

Figure 4. (a) and (b) ATR-FTIR spectra deconvolution of the fully deuterated amide I band (determined at 25 °C at a protein concentration of 100 μM), and (c) and (d) their respective second derivatives. (a) and (c) the e-gp41 in acidic aqueous solution; (b) and (d), membrane-bound e-gp41. The component peaks are the result of a curve fitting using a Gauss line shape. The amide I frequencies characteristic of the various secondary-structure elements were taken from Jackson & Mantsch.[27] The sums of the fitted components superimpose on the experimental amide I region spectra. The black lines represent the experimental FTIR spectra after Savitzky-Golay smoothing; the color lines represent the fitted components of the spectra.

does not result in the dissociation of e-gp41 trimers to a significant extent.

Determination of membrane-induced changes in the secondary structure of e-gp41 by ATR-FTIR spectroscopy

The 3D structure of e-gp41 in the absence of membranes has been determined by solution NMR spectroscopy.[26] Here, we determined the IR spectra of e-gp41 in aqueous solution and when bound to membranes by ATR-FTIR spectroscopy. If membrane binding induces a conformational change that affects the secondary structure of e-gp41 significantly, a comparison of the two spectra will reflect it. Figure 4(a) depicts the spectra of e-gp41 in aqueous solution and (b) in the presence of membranes, and their respective second derivatives calculated to identify the component peaks. The peaks were assigned to the different secondary structural elements, according to Jackson & Mantsch,[27] and the percentage for each element was calculated (see Table 1). The two spectra are very similar: the main component

Table 1. Secondary structure content (%) determined by ATR-FTIR spectroscopy

	α-Helix (~1650 cm^{-1})	β-Strand (1630–1635 cm^{-1})	Aggregated strands (~1625 cm^{-1})	Extended helix/turns (~1625 cm^{-1})	Turns (~1678 cm^{-1})
−Lipids	76 ± 6	4 ± 2	–	8 ± 5	12 ± 1
+Lipids	68 ± 1	9 ± 1	7 ± 1	10 ± 1	6 ± 1

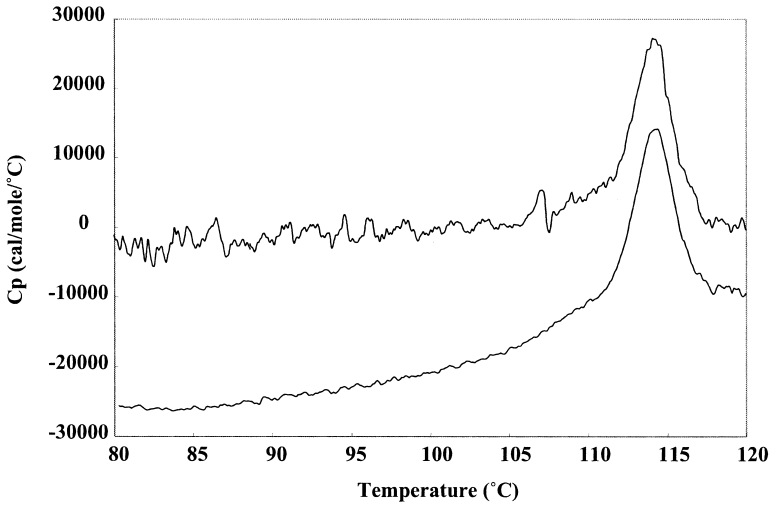

Figure 5. Thermal unfolding of soluble and membrane-bound e-gp41 by DSC. E-gp41 (20 μM) alone (lower trace) and membrane bound at a [e-gp41]/[lipid] ratio of 1:1000 (upper trace) in PBS. In both cases, the heating scan rate was 1.5 deg. C/minute. Traces are displaced arbitrarily along the ordinate for ease of presentation. The thermodynamic parameters derived from these curves (as well as those performed at pH 3.0 or after removal of the loop by mild treatment with trypsin) are listed in Table 2.

corresponds to α-helical structure, with minor components arising from turns and strands that might arise from the immunogenic loop that connects each NHR/CHR pair. The only difference between the two spectra is the presence of an additional peak that accounts for about 7% of the total area, corresponding to aggregated strands in the presence of lipids. It is possible that part of the strand/turns (or part of the population) form tighter interactions in the presence of lipids or that, under the conditions used for the experiment, some protein aggregation occurred.

Determination of membrane-induced changes in the stability of e-gp41 by differential scanning calorimetry (DSC)

The stability of a protein depends on its tertiary structure. Thus, it could be possible to detect significant membrane-induced conformational changes in e-gp41 by comparing the stability of the protein in the presence and in the absence of membranes. Here, we have determined the unfolding temperature of e-gp41 in aqueous solution and when bound to membranes by DSC. In both cases the protein concentration was 20 μM (in PBS) and the heating scan rate was 1.5 deg. C/minute. When necessary, the protein and the lipids (1:1000 molar ratio) were pre-incubated for two hours to ensure full binding. Two representative heating scans (pH 7.3, without lipids, lower trace; with lipids, upper trace) are presented in Figure 5. As observed, the t_m and the shape of the curves are very similar, indicating that, at pH 7.3 e-gp41 is very stable both in the absence and in the presence of lipids. The transition of e-gp41 is only partially reversible; however, such protein denaturation transitions are frequently analyzed assuming that there is a rapid, reversible step (denaturation), followed by an irreversible transition (aggregation).[28] We have used this assumption to estimate the calorimetric transition enthalpy (ΔH_{cal}). The shape of the DSC transition was also used to calculate the values of the van't Hoff enthalpy (ΔH_{vH}) and, from the ratio $\Delta H_{vH}/\Delta H_{cal}$, the cooperative size unit (C.U.). As given in Table 2, e-gp41 is extremely resistant to thermal denaturation under all the conditions tested. In particular, at pH 7.3 the t_m is ~114 °C and the C.U. close to 3, indicating that e-gp41 is preferentially trimeric and denatures in a cooperative manner. At low pH, when no higher-order oligomers are present, the t_m goes down slightly (~110 °C) and the C.U. remains close to 3. Again, there is no difference between soluble e-gp41 and membrane-bound-e-gp41. Furthermore, removal of the loop by

Table 2. Thermodynamic parameters calculated from the DSC curves

pH		Experimental data		Fitting			
		t_m (°C)	ΔH_{cal} (kcal/mol)	t_m (°C)	ΔH_{cal} (kcal/mol)	ΔH_{vH} (kcal/mol)	C.U.
7.3	−Lipids	114.05	88.4	113.9 ± 0.2	84.2 ± 0.9	353 ± 5	3.99
	+Lipids	114.22	98.5	114.1 ± 0.1	93.0 ± 0.7	324 ± 3	3.29
	−Lipids + Trypsin	103.62	100	103.6 ± 0.4	100 ± 1	178 ± 2	1.78
		102.01[a]	58	102.0 ± 0.4	58.0 ± 0.5	126 ± 1	2.17
	+Lipids + Trypsin	102.45	77.6	102.0 ± 0.4	75 ± 1	190 ± 4	2.45
3.0	−Lipids	110.98	110.9	110.7 ± 0.2	107.0 ± 0.2	311 ± 4	2.91
	+Lipids	109.0	104.8	109.0 ± 0.1	102.0 ± 0.6	303 ± 3	2.97

[a] Parameters corresponding to the second heating scan.

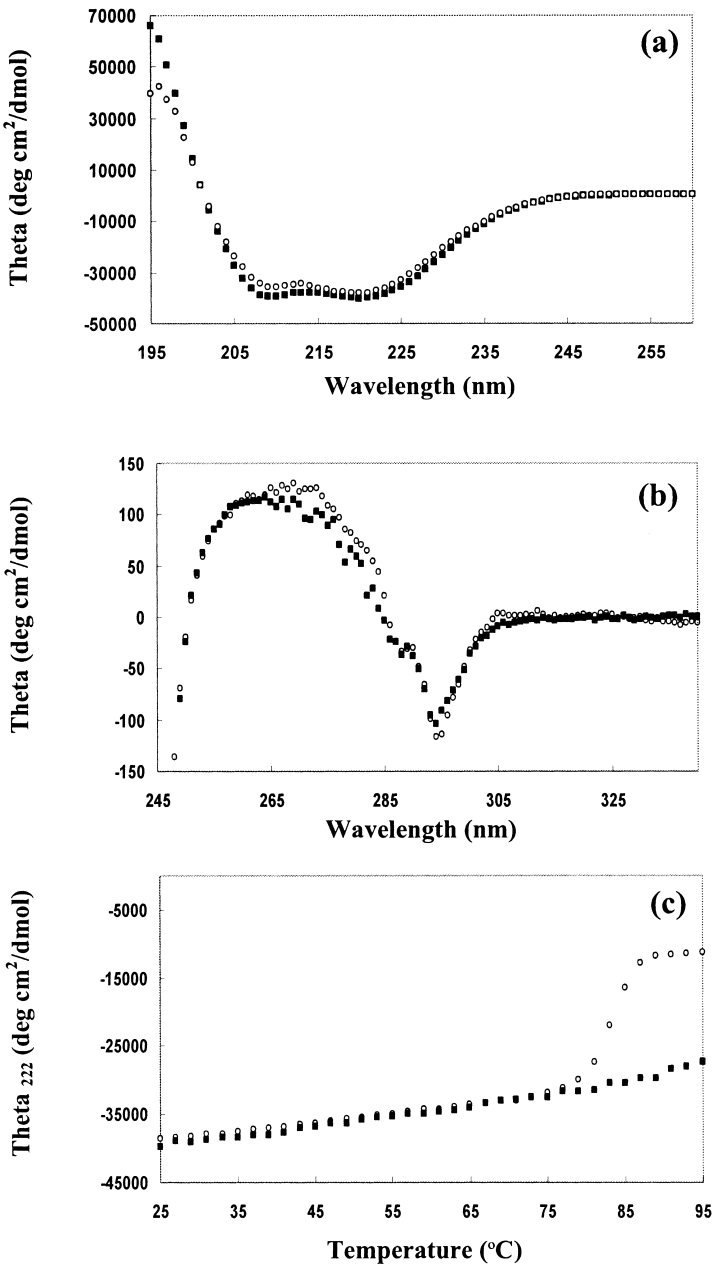

Figure 6. Comparison between the secondary structure, Trp environment, and thermal stability of e-gp41 and cys-e-gp41. (a) Far-UV spectra of e-gp41 and cys-e-gp41, at 15 μM in 50 mM sodium formate (pH 3.0), 100 μM DTT, at 25 °C. (b) Near-UV spectra of e-gp41 and cys-e-gp41, at 60 μM in 50 mM sodium formate (pH 3.0), 100 μM DTT, 25 °C. (c) Thermal unfolding of e-gp41 and cys-e-gp41, 15 μM in 50 mM sodium formate (pH 3.0), 100 μM DTT. Symbols: e-gp41, filled squares; cys-e-gp41, open squares.

Trypsin decreases the t_m to ~103 °C, indicating that covalent attachment of the NHR and CHR segments increases the stability of the helical hairpin. In addition, as indicated in Table 2, removal of the loop results in a substantially reversible unfolding: the t_m observed in the second heating scan is essentially identical with that observed in the first scan, although the ΔH_{cal} is smaller (indicating that only part of the population actually had refolded). Remarkably, the presence of the lipids did not alter the t_m but prevented this refolding (no unfolding peak was observed in the second heating scan in this case). This suggests that binding to the lipids did not alter the structure of the NHR/CHR complex, but after they reached the melting temperature, the membrane-bound free peptides could not re-associate.

Determination of membrane-induced conformational changes in e-gp41 and cys-e-gp41 by Rho fluorescence

The main difference between the model represented by the hexameric complex formed by the NHR and CHR peptides and e-gp41 is that in the latter the NHR and CHR regions are covalently connected by the immunogenic loop. Thus, if the loop restricts the relative movement of NHR and CHR, it could be possible that the putative conformational changes are actually localized at the side of the molecule opposed to the loop, i.e. at the N terminus of NHR and C terminus of CHR. In order to explore this possibility, we labeled the N terminus of e-gp41 with Rho. In the trimeric e-gp41, the internal coiled-coil formed by

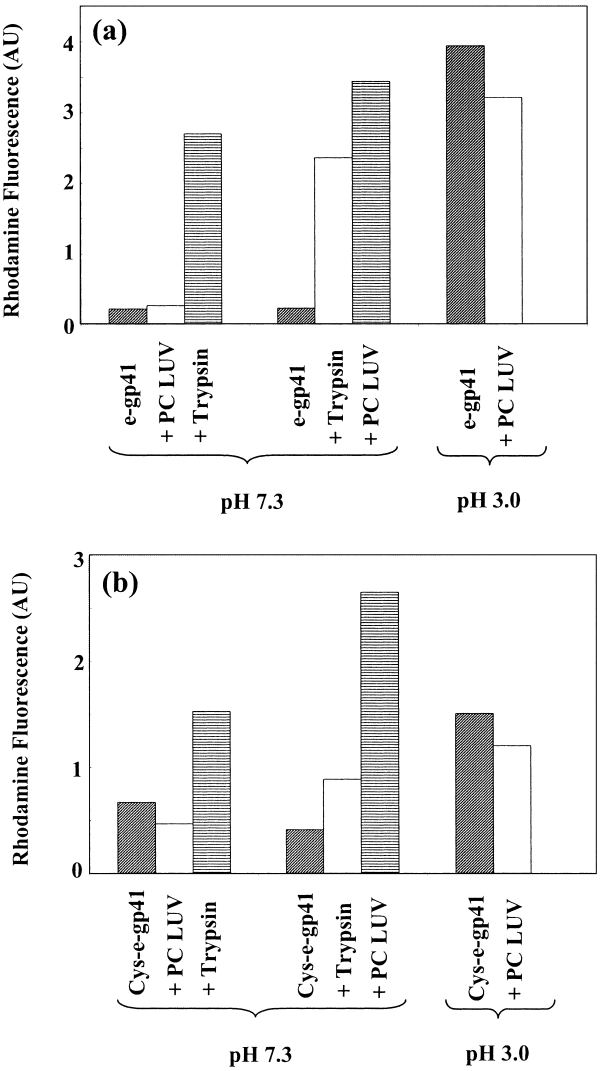

Figure 7. Changes in rhodamine fluorescence of Rho-e-gp41 and Rho-cys-e-gp41 upon membrane binding (all experiments were done at 25 °C). (a) In the first set of experiments, Rho-e-gp41 was fast-diluted to 3 μM in PBS (column 1), then PC LUV were added (final [Rho-e-gp41]/[lipid] ratio of 1:1000; column 2), finally trypsin was added (column three). In the second set of experiments, Rho-e-gp41 was fast-diluted to 3 μM in PBS (column 4), then Trypsin was added (column 5), and finally PC LUV, prepared in PBS, were added (final [Rho-e-gp41]/[lipid] ratio of 1:1000; column 6). In the third set of experiments, Rho-e-gp41 was diluted to 3 μM into 50 mM sodium formate, pH 3.0 (column 7) and then PC LUV, prepared in 50 mM sodium formate (pH 3.0) were added (column eight). (b) In the first set of experiments, Rho-cys-e-gp41 was diluted rapidly to 3 μM in PBS (column 1), then PC LUV were added (final [Rho-cys-e-gp41]/[lipid] ratio of 1:1000; column 2); finally, trypsin was added (column 3). In the second set of experiments, Rho-cys-e-gp41 was diluted rapidly to 3 μM in PBS (column 4), then trypsin was added (column 5), and finally PC LUV, prepared in PBS, were added (final [Rho-cys-e-gp41]/[lipid] ratio of 1:1000; column 6). In the third set of experiments, Rho-cys-e-gp41 was diluted to 3 μM into 50 mM sodium formate, pH 3.0 (column 7) and then PC LUV, prepared in 50 mM sodium formate (pH 3.0) were added (column 8). In all cases, excitation was set at 530 nm (4 nm slit-width), and emission at 580 nm (4 nm slit-width).

three copies of the NHR places three N termini very close to one another. Rho fluorescence is very sensitive to self-quenching. Thus, in the helical hairpin conformation, three Rho molecules attached to the N termini of trimeric e-gp41 are in close proximity, resulting in low fluorescence intensity. If membrane binding induces a conformational change that moves the N termini apart, the Rho molecules would be less quenched and their fluorescence should increase. We used two different strategies to link one Rho molecule to the N terminus of each e-gp41. In the first strategy, we labeled the free amine at the N terminus with Rho succinimidyl-ester (thus linking the Rho molecule directly to the protein backbone). In the second strategy, we elongated e-gp41 four residues towards the N terminus (LTLT in SIVmac239) and added an extra Cys to the N terminus (in the original sequence there is a, not well conserved, Ser in that position), resulting in a new construct, cys-e-gp41. The side-chain of the Cys was then labeled with Rho maleimide. Before the labeling, we determined that elongation of e-gp41 and addition of Cys did not alter the structure of e-gp41. As shown in Figure 6(a), both e-gp41 and cys-e-gp41 have similar secondary structures. Furthermore, as shown in Figure 6(b), their Trp are located in similar environments, suggesting similar tertiary/quaternary structures. The only difference observed is that cys-e-gp41 is less stable than e-gp41 against thermal denaturation (Figure 6(c)). After concluding that cys-e-gp41 folds into the proper conformation, we labeled both proteins with Rho and determined, by mild treatment with trypsin, that the labeling did not alter the conformation of both proteins (i.e. in both cases proteolysis resulted in a Rho-labeled resistant core, data not shown).

In the first set of experiments, Rho-e-gp41 or Rho-cys-e-gp41 were rapidly diluted to a final concentration of 3 μM in PBS and changes in Rho fluorescence were measured following the addition of PC LUV (final protein to lipid ratios 1:1000). As shown in Figure 7, in the first two columns of (a), for e-gp41, and in the first two columns of (b), for cys-e-gp41, membrane binding did not result in significant changes in the intensity of the Rho fluorescence. On the contrary, as shown in column 3, (a) for e-gp41 and (b) for cys-gp41, removal of the loops by mild treatment with trypsin of membrane-bound e-gp41 and cys-e-gp41 resulted in a significant increase in the Rho fluorescence. In the second set of experiments, treatment with trypsin was done before the proteins were bound to membranes (columns 4 and 5, (a) for e-gp41 and (b) for cys-e-gp41). The increase in Rho fluorescence upon removal of the loops suggests that, at pH 7.3 and 3 μM, both e-gp41 and cys-e-gp41 form higher-order oligomers. Subsequent addition of lipids further increases the Rho fluorescence (column 6, (a) for e-gp41 and (b) for cys-e-gp41). Finally, in order to determine if the presence of higher-order oligomers was preventing a

membrane-induced conformational change, we performed an experiment identical with the first set described, but in 50 mM sodium formate (pH 3.0), conditions at which e-gp41 is trimeric and does not further aggregate. As depicted in columns 7 and 8, (a) for e-gp41 and (b) for cys-e-gp41, addition of lipids did not result in a significant increase of the Rho fluorescence, suggesting that at both pH values membrane binding does not significantly alter the distances between the N termini of the three e-gp41 molecules that form each trimer.

Discussion

Understanding the mechanism of virus-induced membrane fusion is basically deciphering how the conformational changes of the viral fusion proteins, triggered by target cell-derived stimuli, are linked to membrane destabilization and merging. Structural analogies with hemagglutinin,[15] the fusion protein of influenza virus, as well as the discovery of peptides derived from the gp41 CHR region that are able to inhibit gp41-mediated virus-cell or cell-cell fusion,[13] suggested that gp41 might adopt several distinctive conformations during the course of fusion. In the native state (whose structure is still unknown), gp41 is associated with gp120. Initially, gp120 binds to CD4, which is presumably located in lipid rafts[29] (although see also Percherancier *et al.*[30]). Subsequent interaction with the co-receptors might require the re-localization of the gp120-CD4 complex outside the rafts,[31] thus the exact lipid composition in which the actual fusion step takes place is still not known. After gp120 binds to the cellular receptors, gp41 projects the N-terminal fusion peptide into the target cell membrane.[10,11] In this hypothetical conformation, called the pre-hairpin intermediate, the N-terminal coiled-coil is formed but the C-terminal helices are not yet packed against its grooves. Later during the fusion process, the pre-hairpin intermediate refolds into the trimeric helical hairpin, bringing the target and viral membrane close to one another. This is the stage represented by the solved structures of a fragment of SIV gp41 ectodomain that includes the NHR and CHR regions, and the loop that connects them (the fragment called here e-gp41), and of a 3:3 complex formed by HIV gp41-derived NHR and CHR peptides,[10–12] all determined in the absence of membranes. Interestingly, when similar HIV gp41-derived NHR/CHR peptide complexes are exposed to lipid bilayers, the core-complex binds to the membrane and dissociates therein.[17] This observation, together with the high membrane-binding affinity that the NHR and the CHR peptides possess, and with their inability to hetero-oligomerize in the membrane surface if they were added independently, led Kliger *et al.*[17] to postulate an additional membrane-induced conformational change in HIV-1 gp41, by which the trimeric helical hairpin binds to the membrane surface and opens. Here, we have further explored this hypothesis by comparing the secondary, tertiary, and quaternary structures and stabilities of soluble and membrane-bound SIV e-gp41 (in which the NHR and CHR regions are covalently linked by the immunogenic loop) by different spectroscopic and calorimetric means. We have chosen SIVmac239 gp41 because it is highly homologous to HIV-1 gp41[32] but it can be expressed and refolded with substantially higher yields than HIV-1 gp41;[33] therefore facilitating its extensive biophysical characterization.

Membrane binding provides the energy required for possible conformational changes

The trimeric helical hairpin is believed to be highly stable. Although the unfolding free energy of SIVmac239 e-gp41 is not known, Lu and co-workers[34] have determined the urea-induced unfolding free energy of SIV N36(L6)C34, a construct corresponding to part of the NHR and CHR regions, lacking the N-terminal fusion peptide and the pre-transmembrane Trp-rich region and in which the original immunogenic loop was replaced by a short SGGRGG sequence. They reported an apparent ΔG° of -17.9 kcal/mol (1 cal = 4.184 J). If membrane binding is expected to result in a conformational change that disturbs the trimeric helical hairpin significantly, it must provide the required energy to do so. Here, we found that the ΔG of membrane binding for e-gp41 is about -10 kcal/mol. Considering that N36(L6)C34 indeed corresponds to the most stable regions of e-gp41 (in particular the more flexible immunogenic loop is not present), we can confidently conclude that the energy available from membrane binding might suffice for, at least, partial conformational changes.

The conformational change observed when the loop is removed is not observed when the loop is present

We found that the energy required for possible conformational changes could be provided by membrane binding. However, we have shown here that membrane binding of trimeric SIVmac239 e-gp41 results neither in dissociation of the trimers nor in significant changes in their structure and stability. There are two differences between the model represented by the HIV-1 derived peptide complex that was shown to dissociate[17] and the SIV e-gp41 studied here that may account for their different behavior. First, although HIV-1 and SIV gp41 are highly homologous (~50% identity in the region corresponding to e-gp41[32]) and their structures have been found to be almost identical,[10–12] the differences in their amino acid sequences, although very unlikely, might still account for the different behavior observed between the HIV-derived peptide complex and the

SIV-derived e-gp41. SIV gp41 contains a four residue deletion in the loop and an Ile at an "a" position in the NHR of HIV-1 gp41 is replaced in SIV by Thr (T586 in SIVmac239 gp41). The presence of this Thr has been postulated to decrease the stability of SIV gp41 trimeric helical hairpin, as compared to the HIV-1 protein. Indeed, the melting temperature of the SIV N36(L6)C34 T586I mutant is 21 deg. C higher than that of the wild type construct.[34] Similarly, replacement of the equivalent wild-type Ile in HIV-1 N36(L6)C34 by Thr lowers the melting temperature from 70 °C to 45 °C.[35] These observations suggest that, indeed, the SIV e-gp41 construct analyzed here is expected to be less stable than its HIV-1 derived counterpart. Thus, it is unlikely that the inability of SIV e-gp41 trimeric helical hairpin to open upon membrane binding arises from a hypothetically higher stability. In addition, it should be noted that the presence of the Thr, instead of the Ile, in SIV gp41 might reduce the membrane binding affinity of the N-terminal coiled-coil, would the helical hairpin dissociate.

The second (and for us more significant) difference between the SIV-gp41 e-gp41 and the HIV-1 gp41-derived peptide complex, is that in the former the NHR and CHR regions are covalently connected by the immunogenic loop. This might imply that the conformational changes observed when the peptide complex was analyzed are somehow restricted when the NHR and CHR segments are connected and, indeed, are localized at the side of the molecule far away from the loop. We tested this hypothesis by analyzing how membrane binding affected the fluorescence of Rho molecules attached to the N terminus of e-gp41. In the trimeric helical hairpin conformation, three Rho molecules are in close proximity and their fluorescence is self-quenched. Had membrane binding induced a significant opening of this region, the distance between the Rho molecules would have increased and the fluorescence should have increased. The observation that addition of trypsin to membrane-bound Rho-e-gp41 (and to Rho-cys-e-gp41) did result in a dequenching of the Rho fluorescence, suggests that when the loop is removed some conformational changes might occur. The fact that in the DSC experiments these changes were not detected (i.e. the t_m of unfolding in the absence or in the presence of the lipids, when the loop had been removed were similar) could be related to the different concentrations required for the Rho fluorescence experiments and the DSC. In the latter, high concentrations were needed to obtain reliable signals. Thus, it is possible that removal of the loop altered the monomer-trimer equilibrium and, at the low concentrations analyzed in the Rho fluorescence experiments, some dissociation of the trimers could have occurred. This might have resulted in an opening of the hairpins or have rendered them susceptible to protease attack, two events that would result in an increase of the Rho fluorescence. In line with this, it has been shown that the 3D structures of HIV-1 N34(L6)C28, determined from crystals grown at high concentrations (~1 mM) of protein in the presence of detergents (SDS or βOG) are similar to that obtained from crystals grown in water.[36] In conclusion, the experimental observations presented here indicate that the immunodominant loop stabilizes the trimeric helical hairpin conformation of SIVmac239 e-gp41.

Although a better model than the NHR/CHR peptide complex, e-gp41 still lacks the N-terminal fusion peptide and the C-terminal Trp-rich region

We should stress that, although e-gp41 is a better model than the NHR/CHR peptide complex for analyzing the structural consequences of gp41-membrane interaction, it still lacks two important regions of the full-length gp41 ectodomain: the N-terminal fusion peptide and the pre-transmembrane Trp-rich region, which, indeed, are expected to interact with the membrane. Whether the stabilizing effect of the loop is enhanced, or on the contrary diminished, when these other regions are part of the molecule is unknown. Interestingly, it has been reported that epitopes corresponding to HIV-1 gp41 NHR and CHR pepides (either when they are part of the pre-hairpin intermediate or of the trimeric helical hairpin), exposed during fusion between cells expressing HIV-1 gp120/gp41 (strain HXB2) and cells expressing CD4/CXCR4, disappear from the cell surface within minutes after fusion has started.[37] This raises the possibility that, in the full-length gp41, a conformational change that alters the epitopes' conformations actually occurs. This might imply that the fusion peptide and Trp-rich regions indeed help to alter gp41 conformation; or that proteases present in the proximity of the membranes of the fusing cells might remove the gp41 loop and thus alter gp41 conformation; two hypotheses that should be addressed in the future by analyzing the interactions between gp41 and cell membranes. Alternatively, it is possible that the epitopes remain intact; but, as fusion proceeds, are no longer exposed to the antibodies. Distinguishing between these hypotheses should be the focus of future investigation.

Materials and Methods

Materials

Egg phosphatidylcholine (PC) and dioleoylphosphatidylcholine (DOPC) were purchased from Lipid Products (South Nutfield, UK). Carboxytetramethylrhodamine (Rho) succinimidyl-ester and tetramethylrhodamine maleimide were purchased from Molecular Probes (Eugene, OR). All other reagents were of analytical grade. Buffers were prepared using double glass-distilled water. Phosphate-buffered saline (PBS) is NaCl

(8 g/l), KCl (0.2 g/l), KH_2PO_4 (0.2 g/l), and Na_2HPO_4 (1.09 g/l), pH 7.3.

Site-directed mutagenesis and protein expression

SIVmac239 e-gp41 (residues 27–149, with Cys86 and Cys92, present in the loop connecting the N and C-terminal heptad repeats, replaced by Ala) was overexpressed from pET 11a (kindly provided by P. T. Wingfield, NIH) in *E. coli* BL21 DE3. Replacement of the Cys facilitated refolding of the protein without altering its physical and biochemical properties.[33] SIV cys-e-gp41 (also with Cys86 and Cys92 replaced by Ala) was obtained by PCR site-directed mutagenesis using the pET 11a-e-gp41 as template. Specifically, e-gp41 was elongated toward the N terminus by adding the corresponding four residues (LTLT in gp41 from SIVmac239) and an extra N-terminal Cys for subsequent labeling with fluorescent probes (in SIVmac239 gp41 this position was occupied by a non-conserved Ser). The PCR fragment (which included the bacteriophage T7 promoter and ribosome binding site sequence from the pET-11a) was ligated by T/A cloning into pGEM-T (Promega). cys-e-gp41 was overexpressed from pGEM-T in *E. coli* BL21 DE3.

Protein purification and labeling with rhodamine

Both e-gp41 and cys-e-gp41 were purified from GuHCl-solubilized inclusion bodies by reversed phase (RP)-HPLC (with a gradient from 25% to 60% (v/v) acetonitrile) and refolded by dialysis against 50 mM sodium formate, pH 3.0 (100 mM DTT in the case of cys-e-gp41) at a very low concentration of protein to prevent aggregation, as described.[18] After dialysis, the aggregates were removed by ultracentrifugation and the proteins were concentrated to about 10 mg/ml by centrifugation through Centricom membranes. The molecular masses of the proteins were confirmed by mass spectrometry. That the proteins were 99% trimeric and no large aggregates were present was confirmed by dynamic light scattering. Protein concentrations were determined by measuring absorbance at 280 nm in 6 M GuHCl.

N-terminal labeling of e-gp41 with Rho was achieved by dissolving pure e-gp41 in *N*,*N*-dimethylformamide (DMF)/tetraethylammonium (TEA) (9.875:0.125) pH 7.0, at about 1 mg/ml of protein, and adding carboxytetramethyl-rhodamine succinimidyl-ester (from a 0.2 mg/ml stock in DMF) to a final concentration of 0.03 mg/ml (thus, the molar ratio of protein to Rho was about 1:1). The reaction, followed by RP-HPLC, was usually completed after 24 hours. The N-terminally Rho-labeled e-gp41 appeared as a new peak (slightly shifted to higher concentrations of acetonitrile and with a spectrum that showed the characteristic Rho absorbance at ~530–560 nm). The peak was purified by RP-HPLC and the addition of one Rho molecule was confirmed by mass spectrometry.

Rho labeling of the Cys side-chain was achieved by incubation of pure cys-e-gp41 in 6 M GuHCl, 0.1 M Na_2HPO_4/NaH_2PO_4 (pH 7.1), with tetramethylrhodamine maleimide (TMR-M, previously dissolved at about 20 mM in dimethylsulfoxide) at final concentrations of 1 mg/ml of TMR-M and 0.75 mg/ml of cys-e-gp41). The reaction, generally completed after about 24 hours, was followed by HPLC. After purification, the addition of one Rho molecule was confirmed by mass spectrometry. The concentrations of Rho-labeled proteins were determined by absorbance at 545 nm in 6 M GuHCl, using a calculated molar extinction coefficient for Rho of 38,000 M^{-1} cm^{-1}.

Preparation of lipid vesicles

Small and large unilamellar vesicles (SUV and LUV, respectively) were prepared from egg-PC or DOPC as follows: dry lipids films were suspended in PBS or 50 mM sodium formate (pH 3.0) by vortex mixing to produce multilamellar vesicles (MLV). SUV were obtained by sonication of the MLV until the solution cleared. LUV were obtained from the MLV by five cycles of freeze and thaw, followed by extrusion (20 passes) through two stacked 0.1 μm-diameter pores (Nuclepore Corp., Pleasanton, CA). SUV and LUV were kept at 4 °C and used within 24 hours.

Membrane partition of e-gp41

SPR experiments, to determine membrane partition, were carried out with a BIAcore 3000 analytical system (Biacore, Uppsala, Sweden) using an HPA sensor chip (Biacore). The running buffer used for all experiments was 50 mM sodium formate (pH 3.0). The washing solution was 40 mM *n*-octyl β-D-glucopyranoside (βOG). The regenerating solution was 10 mM NaOH. All solutions were freshly prepared, degassed, and filtered through 0.22 μm-diameter pore Nucleopore filters. The operating temperature was 25 °C. The HPA chip was then installed and cleaned by an injection of the non-ionic detergent βOG(25 μl, 40 mM), at a flow-rate of 5 μl/minute. PC SUVs (80 μl, 0.5 mM) were then applied to the chip surface at a low flow-rate (2 μl/minute). To remove any multilamellar structures from the lipid surface, NaOH (50 μl, 10 mM) was injected at a flow-rate of 50 μl/minute, which resulted in a stable baseline corresponding to the lipid monolayer linked to the chip surface. After the baseline was stable, 15 μl of e-gp41 (in the range from 134 nM to 13.4 μM) in 50 mM sodium formate (pH 3.0) were injected on the lipid surface at a flow-rate of 5 μl/minute. Note that, because e-gp41 should be dissolved in the running buffer for several hours before it encounters the lipid membrane, low pH should be used to ensure that e-gp41 does not form large aggregates[38] that might damage the chip. Indeed, the structure of fragments from gp41 determined either at pH 3.0 or at neutral pH were very similar, indicating that low pH does not alter gp41 conformation.[10,11] Buffer alone then replaced the protein solution for 15 minutes to allow protein dissociation. SPR detects changes in the reflective index of the surface layer of lipids in contact with the sensor chip. A sensogram is obtained by plotting the SPR angle against time. Analysis of the protein–lipid binding event was performed from a series of sensograms collected at several different concentrations of peptide. Our system reached binding equilibrium during sample injection and therefore the affinity constant could be calculated from the relationship between the equilibrium binding response and the concentration of protein, using a steady-state affinity model. The affinity constants were derived from the following equation (by non-linear, least-squares fitting):

$$\text{R.U.}i = (K_A[\text{e-gp41}]i\text{R.U.}^{\text{MAX}})/(K_A[\text{e-gp41}]i + 1)$$

where R.U. *i* is the signal measured, [e-gp41]*i* is the *i* concentration of e-gp41, R.U.^{MAX} is the maximal response unit (or equilibrium binding response), and K_A is the

affinity constant. The free energy (ΔG) was calculated according to $\Delta G = -RT \ln([H_2O]K_A)$. The universal gas constant was taken as $R = 1.987$ cal/(K mol) and the concentration of water is 55.556 M.

Determination of membrane-induced changes in the oligomeric state of e-gp41 by Trp fluorescence

The fluorescence of Trp depends on the polarity of its environment. Thus, changes in oligomeric state that affect the Trp environment might result in changes in Trp fluorescence. We determined the fluorescence of membrane-bound e-gp41 Trp in the range of [e-gp41] from 0.2 μM (the concentration at which e-gp41 is >90% monomeric) to 5 μM (the concentration at which e-gp41 is >90% trimeric). In all cases, e-gp41 was pre-incubated in 50 mM sodium formate (pH 3.0) at the desired concentration for 24 hours to ensure the corresponding equilibrium monomer–trimer was reached (this prevented us from doing this experiment at pH 7.3). Then PC SUV (prepared in 50 mM sodium formate, pH 3.0) were added at a final [e-gp41]/[lipid] ratio of 1:1000 and incubated for another two hours to ensure full binding before measuring the fluorescence. Measurements were done in an SLM-Aminco Series 2 spectrophotometer in a quartz cuvette with excitation at 280 nm (4 nm slit-width) and emission in the range 300–400 nm, at 25 °C. The spectra of the corresponding amounts of lipids alone were subtracted.

Determination of membrane-induced changes in the secondary structure of e-gp41 by FTIR spectroscopy

Spectra were obtained with a Bruker equinox 55 FTIR spectrometer equipped with a deuterated triglyceride sulfate (DTGS) detector and coupled with an ATR device. For each spectrum, 150 scans were collected, with resolution of 4 cm^{-1}. Samples were prepared as described.[39] Briefly, PC (0.78 mg) was dissolved in methanol and deposited on a ZnSe horizontal ATR prism (80 mm × 7 mm) by spreading with a Teflon bar. Drying under vacuum for 30 minutes eliminated the solvents. Previous to sample preparations, the trifluoroacetate (CF_3COO^-) counterions, which might associate with the protein during HPLC purification, were replaced with chloride ions through several washings of the proteins in 0.1 M HCl and lyophilizations. This allowed the elimination of the strong C=O stretching absorption band near 1673 cm^{-1}.[40] e-gp41 was then refolded in 50 mM sodium formate (pH 3.0), centrifuged to remove aggregates and dialyzed against deuterium oxide (^2H_2O) (slightly acidified to pH 4 to prevent protein aggregation) for 48 hours and added to the surface of the naked prism or a prism covered with the PC membranes at a final protein concentration of 100 μM. Polarized spectra were recorded at 25 °C and the respective spectra corresponding to pure phospholipids (covered with acidified ^2H_2O) in each polarization were subtracted from the sample spectra to yield the difference spectra. The background for each spectrum was a clean ZnSe prism.

Prior to curve fitting, a straight base-line passing through the ordinates at 1700 cm^{-1} and 1600 cm^{-1} was subtracted. To resolve overlapping bands, the spectra were processed using PEAKFIT™ (Jandel Scientific, San Rafael, CA) software. Second-derivative spectra were calculated to identify the positions of the component bands in the spectra. These wavenumbers were used as initial parameters for curve fitting with gaussian component peaks. Position, bandwidths, and amplitudes of the peaks were varied until good agreement between the calculated sum of all components and the experimental spectra were achieved ($r^2 > 0.995$), under the following restraints: (i) the resulting bands shifted by no more than 2 cm^{-1} from the initial parameters; and (ii) all the peaks had reasonable half-widths (<20–25 cm^{-1}). The relative contents of different secondary structure elements were estimated by dividing the areas of individual peaks, assigned to particular secondary structure, by the whole area of the resulting amide I band. The experiments were repeated twice and were found to be in good agreement.

Determination of membrane-induced changes in the stability of e-gp41 by differential scanning calorimetry (DSC)

A VP-DSC instrument from the MicroCal Corp. (Northampton, MA) was used for all scans. For scanning e-gp41 in the absence of lipids at pH 7.3, the protein was first diluted to 20 μM in PBS (from a 10 mg/ml stock in 50 mM sodium formate, pH 3.0), then degassed and loaded into the calorimeter sample cell. For the experiments done at pH 3.0, the protein was diluted to 20 μM in 50 mM sodium formate (pH 3.0). The corresponding buffer was placed in the reference cell. For the scans in the presence of lipids (DOPC was used to ensure that no lipid phase transitions occur within the range of temperatures analyzed), e-gp41 and DOPC LUV were pre-incubated at a ratio of 1:1000 (20 μM e-gp41) in PBS (or in 50 mM sodium formate (pH 3.0), depending on the desired pH) for two hours to ensure full binding, then degassed and loaded into the sample cell. Now DOPC LUV (prepared in PBS or in the sodium formate buffer, as required) at the corresponding concentration were placed in the reference cell. For the experiments in which the loop was removed, e-gp41 (alone or membrane-bound) was incubated with trypsin (final concentration of 7 μg/ml) for two hours prior to the DSC experiment. Heating scan rates of 1.5 deg. C/minute and cooling scan rates of 1 deg. C/minute were used. The e-gp41 transition was fitted using parameters to describe an equilibrium with a single van't Hoff enthalpy. Data were analyzed with the program Origin 5.0.

Determination of the secondary structure, Trp environment, and thermal stability of cys-e-gp41 by circular dichroism (CD)

The far-UV and near-UV CD spectra of e-gp41 and its thermal stability have been reported.[33] To determine whether cys-e-gp41 adopted the correct gp41 conformation after refolding, the far-UV and near-UV CD spectra of cys-e-gp41 were determined and compared to those of e-gp41. Furthermore, the stability of cys-e-gp41 against thermal denaturation was assessed by CD and compared to that of e-gp41. Specifically, the far-UV spectrum of e-gp41 and cys-e-gp41, at 15 μM in 50 mM sodium formate (pH 3.0), 100 μM DTT, were determined in an Aviv 202 spectropolarimeter, in a capped quartz optical cell with a 1 mm path-length, at 25 °C, in the range of 195–260 nm in 1 nm steps with an averaging time of ten seconds. The near-UV spectrum of e-gp41 and cys-e-gp41, at 60 μM in 50 mM sodium formate (pH 3.0), 100 μM DTT, were determined in a capped quartz

optical cell with a 1 cm path length, at 25 °C, in the range of 240–340 nm with 1 nm steps and an averaging time of two seconds. The stabilities of e-gp41 and cys-e-gp41 (15 μM in 50 mM sodium formate (pH 3.0), 100 μM DTT) against thermal denaturation were determined by measuring the CD signal at 222 nm (characteristic of their highly helical structure) as a function of the temperature, in the range of 10–95 °C with 2 deg. C steps, at a heating rate of 2 deg. C/minute with an equilibration time of two minutes at each temperature and an averaging time of ten seconds.

Determination of membrane-induced conformational changes in e-gp41 and cys-e-gp41 by rhodamine fluorescence

Rhodamine fluorescence is highly sensitive to self-quenching but affected only weakly by the dielectric constant of its environment. Therefore, possible membrane-induced conformational changes that move the N termini of gp41 trimers away from each other can be studied by monitoring the Rho fluorescence of N-terminally Rho-labeled gp41. Specifically, we analyzed two different Rho-labeled gp41 constructs: (i) Rho-e-gp41, in which the Rho molecule was linked to the free N terminus of e-gp41; and (ii) Rho-cys-e-gp41, in which the Rho molecule was linked to the side-chain of a Cys residue added to the N terminus of an elongated e-gp41. Rho-e-gp41 or Rho-cys-e-gp41 were fast diluted to a final concentration of 3 μM from concentrated stocks in 50 mM sodium formate (pH 3.0) into a quartz cuvette containing 400 μl of PBS at 25 °C. In the first set of experiments, changes in Rho fluorescence were measured following the addition of PC LUV prepared in PBS (final protein/lipid ratio 1:1000). After the fluorescence was stable (to ensure that full binding was achieved and that possible conformational changes were completed), 10 μl of 1 mg/ml of trypsin were added to the cuvette and the Rho fluorescence was measured until the system stabilized. In the second set of experiments, the trypsin was added to either Rho-e-gp41 or Rho-cys-e-gp41 first and only after the fluorescence leveled off were the PC LUV added. In the third set of experiments, Rho-e-gp41 or Rho-cys-e-gp41 were incubated at a final concentration of 3 μM in 50 mM sodium formate (pH 3.0) and, after the fluorescence was stable, the PC LUV now prepared in 50 mM sodium formate, pH 3.0 (final protein/lipid ratio 1:1000) were added. In all cases, excitation was set at 530 nm (4 nm slit-width), and emission at 580 nm (4 nm slit-width).

Acknowledgements

We are indebted to R. Blumenthal, A. DeVico, and M. Lu for their comments on the manuscript. S.G.P. is supported by fellowships from The Mifal Ha'paiys Foundation of Israel and the Feinberg Graduate School.

References

1. Dalgleish, A. G., Beverley, P. C., Clapham, P. R., Crawford, D. H., Greaves, M. F. & Weiss, R. A. (1984). The CD4 (T4) antigen is an essential component of the receptor for the AIDS retrovirus. *Nature*, **312**, 763–767.
2. Alkhatib, G., Combadiere, C., Broder, C. C., Feng, Y., Kennedy, P. E., Murphy, P. M. & Berger, E. A. (1996). CC CKR5: a RANTES, MIP-1alpha, MIP-1beta receptor as a fusion cofactor for macrophage-tropic HIV-1. *Science*, **272**, 1955–1958.
3. Feng, Y., Broder, C. C., Kennedy, P. E. & Berger, E. A. (1996). HIV-1 entry cofactor: functional cDNA cloning of a seven-transmembrane, G protein-coupled receptor. *Science*, **272**, 872–877.
4. Bosch, M. L., Earl, P. L., Fargnoli, K., Picciafuoco, S., Giombini, F., Wong-Staal, F. & Franchini, G. (1989). Identification of the fusion peptide of primate immunodeficiency viruses. *Science*, **244**, 694–697.
5. Gallaher, W. R. (1987). Detection of a fusion peptide sequence in the transmembrane protein of human immunodeficiency virus. *Cell*, **50**, 327–328.
6. Harter, C., James, P., Bachi, T., Semenza, G. & Brunner, J. (1989). Hydrophobic binding of the ectodomain of influenza hemagglutinin to membranes occurs through the "fusion peptide". *J. Biol. Chem.* **264**, 6459–6464.
7. Gallaher, W. R., Ball, J. M., Garry, R. F., Griffin, M. C. & Montelaro, R. C. (1989). A general model for the transmembrane proteins of HIV and other retroviruses. *AIDS Res. Hum. Retroviruses*, **5**, 431–440.
8. Blacklow, S. C., Lu, M. & Kim, P. S. (1995). A trimeric subdomain of the simian immunodeficiency virus envelope glycoprotein. *Biochemistry*, **34**, 14955–14962.
9. Lu, M., Blacklow, S. C. & Kim, P. S. (1995). A trimeric structural domain of the HIV-1 transmembrane glycoprotein. *Nature Struct. Biol.* **2**, 1075–1082.
10. Chan, D. C., Fass, D., Berger, J. M. & Kim, P. S. (1997). Core structure of gp41 from the HIV envelope glycoprotein. *Cell*, **89**, 263–273.
11. Weissenhorn, W., Dessen, A., Harrison, S. C., Skehel, J. J. & Wiley, D. C. (1997). Atomic structure of the ectodomain from HIV-1 gp41. *Nature*, **387**, 426–430.
12. Caffrey, M., Cai, M., Kaufman, J., Stahl, S. J., Wingfield, P. T., Covell, D. G. *et al.* (1998). Three-dimensional solution structure of the 44 kDa ectodomain of SIV gp41. *EMBO J.* **17**, 4572–4584.
13. Wild, C. T., Shugars, D. C., Greenwell, T. K., McDanal, C. B. & Matthews, T. J. (1994). Peptides corresponding to a predictive alpha-helical domain of human immunodeficiency virus type 1 gp41 are potent inhibitors of virus infection. *Proc. Natl Acad. Sci. USA*, **91**, 9770–9774.
14. Bullough, P. A., Hughson, F. M., Skehel, J. J. & Wiley, D. C. (1994). Structure of influenza haemagglutinin at the pH of membrane fusion. *Nature*, **371**, 37–43.
15. Skehel, J. J. & Wiley, D. C. (1998). Coiled coils in both intracellular vesicle and viral membrane fusion. *Cell*, **95**, 871–874.
16. Furuta, R. A., Wild, C. T., Weng, Y. & Weiss, C. D. (1998). Capture of an early fusion-active conformation of HIV-1 gp41. *Nature Struct. Biol.* **5**, 276–279.
17. Kliger, Y., Peisajovich, S. G., Blumenthal, R. & Shai, Y. (2000). Membrane-induced conformational change during the activation of HIV-1 gp41. *J. Mol. Biol.* **301**, 905–914.
18. Peisajovich, S. G. & Shai, Y. (2001). SIV gp41 binds to membranes both in the monomeric and trimeric states: consequences for the neuropathology and inhibition of HIV infection. *J. Mol. Biol.* **311**, 249–254.
19. Ben-Efraim, I., Kliger, Y., Hermesh, C. & Shai, Y. (1999). Membrane-induced step in the activation

of Sendai virus fusion protein. *J. Mol. Biol.* **285**, 609–625.
20. Epand, R. F., Macosko, J. C., Russell, C. J., Shin, Y. K. & Epand, R. M. (1999). The ectodomain of HA2 of influenza virus promotes rapid pH dependent membrane fusion. *J. Mol. Biol.* **286**, 489–503.
21. Ghosh, J. K. & Shai, Y. (1999). Direct evidence that the N-terminal heptad repeat of Sendai virus fusion protein participates in membrane fusion. *J. Mol. Biol.* **292**, 531–546.
22. Peisajovich, S. G., Samuel, O. & Shai, Y. (2000). The F1 protein of paramyxoviruses has two fusion peptides: implications for the mechanism of membrane fusion. *J. Mol. Biol.* **296**, 1353–1365.
23. Suarez, T., Gallaher, W. R., Agirre, A., Goni, F. M. & Nieva, J. L. (2000). Membrane interface-interacting sequences within the ectodomain of the human immunodeficiency virus type 1 envelope glycoprotein: putative role during viral fusion. *J. Virol.* **74**, 8038–8047.
24. Caffrey, M., Kaufman, J., Stahl, S., Wingfield, P., Gronenborn, A. M. & Clore, G. M. (1999). Monomer–trimer equilibrium of the ectodomain of SIV gp41: insight into the mechanism of peptide inhibition of HIV infection. *Protein Sci.* **8**, 1904–1907.
25. Kliger, Y., Gallo, S. A., Peisajovich, S. G., Munoz-Barroso, I., Avkin, S., Blumenthal, R. & Shai, Y. (2001). Mode of action of an antiviral peptide from HIV-1. Inhibition at a post-lipid mixing stage. *J. Biol. Chem.* **276**, 1391–1397.
26. Caffrey, M., Cai, M., Kaufman, J., Stahl, S. J., Wingfield, P. T., Gronenborn, A. M. & Clore, G. M. (1997). Determination of the secondary structure and global topology of the 44 kDa ectodomain of gp41 of the simian immunodeficiency virus by multidimensional nuclear magnetic resonance spectroscopy. *J. Mol. Biol.* **271**, 819–826.
27. Jackson, M. & Mantsch, H. H. (1995). The use and misuse of FTIR spectroscopy in the determination of protein structure. *Crit. Rev. Biochem. Mol. Biol.* **30**, 95–120.
28. Epand, R. F., Epand, R. M. & Jung, C. Y. (2001). Ligand-modulation of the stability of the glucose transporter GLUT 1. *Protein Sci.* **10**, 1363–1369.
29. Del Real, G., Jimenez-Baranda, S., Lacalle, R. A., Mira, E., Lucas, P., Gomez-Mouton, C. *et al.* (2002). Blocking of HIV-1 infection by targeting CD4 to non-raft membrane domains. *J. Exptl Med.* **196**, 293–301.
30. Percherancier, Y., Lagane, B., Planchenault, T., Staropoli, I., Altmeyer, R., Virelizier, J. L. *et al.* (2002). HIV-1 entry into T-cells is not dependent on CD4 and CCR5 localization to sphingolipid-enriched, detergent-resistant, raft membrane domains. *J. Biol. Chem.* **12**, 00 epub ahead of printing on Nov. 12 as Manuscript M207371200..
31. Kozak, S. L., Heard, J. M. & Kabat, D. (2002). Segregation of CD4 and CXCR4 into distinct lipid microdomains in T lymphocytes suggests a mechanism for membrane destabilization by human immunodeficiency virus. *J. Virol.* **76**, 1802–1815.
32. Caffrey, M. (2001). Model for the structure of the HIV gp41 ectodomain: insight into the intermolecular interactions of the gp41 loop. *Biochim. Biophys. Acta*, **1536**, 116–122.
33. Wingfield, P. T., Stahl, S. J., Kaufman, J., Zlotnick, A., Hyde, C. C., Gronenborn, A. M. & Clore, G. M. (1997). The extracellular domain of immunodeficiency virus gp41 protein: expression in *Escherichia coli*, purification, and crystallization. *Protein Sci.* **6**, 1653–1660.
34. Ji, H., Bracken, C. & Lu, M. (2000). Buried polar interactions and conformational stability in the simian immunodeficiency virus (SIV) gp41 core. *Biochemistry*, **39**, 676–685.
35. Liu, J., Shu, W., Fagan, M. B., Nunberg, J. H. & Lu, M. (2001). Structural and functional analysis of the HIV gp41 core containing an Ile573 to Thr substitution: implications for membrane fusion. *Biochemistry*, **40**, 2797–2807.
36. Shu, W., Ji, H. & Lu, M. (2000). Interactions between HIV-1 gp41 core and detergents and their implications for membrane fusion. *J. Biol. Chem.* **275**, 1839–1845.
37. Finnegan, C. M., Berg, W., Lewis, G. K. & DeVico, A. L. (2002). Antigenic properties of the human immunodeficiency virus transmembrane glycoprotein during cell–cell fusion. *J. Virol.* **76**, 12123–12134.
38. Caffrey, M., Braddock, D. T., Louis, J. M., Abu-Asab, M. A., Kingma, D., Liotta, L. *et al.* (2000). Biophysical characterization of gp41 aggregates suggests a model for the molecular mechanism of HIV-associated neurological damage and dementia. *J. Biol. Chem.* **275**, 19877–19882.
39. Gazit, E., Miller, I. R., Biggin, P. C., Sansom, M. S. & Shai, Y. (1996). Structure and orientation of the mammalian antibacterial peptide cecropin P1 within phospholipid membranes. *J. Mol. Biol.* **258**, 860–870.
40. Surewicz, W. K., Mantsch, H. H. & Chapman, D. (1993). Determination of protein secondary structure by Fourier transform infrared spectroscopy: a critical assessment. *Biochemistry*, **32**, 389–394.

Edited by G. von Heijne

(Received 29 October 2002; received in revised form 12 December 2002; accepted 20 December 2002)